Applied Physics Research; Vol. 8, No. 4; 2016
ISSN 1916-9639 E-ISSN 1916-9647
Published by Canadian Center of Science and Education

Numerical Investigation of Mid-Infrared Supercontinuum Generation in GeAsSe Based Chalcogenide Photonic Crystal Fiber Using Low Peak Power

M. R. Karim[1] & B. M. A. Rahman[1]

[1] School of Mathematics, Computer Science and Engineering, City University London, London, EC1V 0HB, UK

Correspondence: M. R. Karim, School of Mathematics, Computer Science and Engineering, City University London, London, EC1V 0HB, UK. Tel: 44-780-925-0505. E-mail: mohammad.karim.2@city.ac.uk

Received: June 11, 2016 Accepted: June 22, 2016 Online Published: July 29, 2016

doi:10.5539/apr.v8n4p29 URL: http://dx.doi.org/10.5539/apr.v8n4p29

Abstract

We numerically investigate the use of photonic crystal fiber (PCF) through dispersion engineering of its cladding containing air-holes for supercontinuum (SC) generation in the mid-infrared region using low peak power. A 3.6-cm-long PCF made using $Ge_{11.5}As_{24}Se_{64.5}$ chalcogenide (ChG) glass with a hexagonal array of air-holes was optimized for obtaining zero-dispersion wavelength through dispersion tailoring around the pump wavelength of 4 μm. We have performed numerical simulations for such dispersion tailored ChG PCF with the peak power range between 0.25 kW and 2 kW. It was found through rigorous numerical simulations that an ultrabroadband mid-infrared SC spectra covering the wavelength range 2-8 μm which is equivalent to 2 octaves could be generated using pump pulses of 320 fs duration at a wavelength of 4 μm with a relatively low peak power of 2 kW by using our proposed ChG PCF design.

Keywords: photonic crystal fiber, nonlinear optics, chalcogenide, supercontinuum generation

1. Introduction

Supercontinuum (SC) generation is a complex spectral broadening process where a narrow bandwidth pulse undergoes a substantial spectral expansion through the interplay between various linear and nonlinear phenomena that occur during the propagation of the optical signal along the length of the waveguide. SC generation using nonlinear effects in optical waveguides has attracted extensive attention in nonlinear optics in the past decade as its use provides an optical source with properties such as large bandwidth, brightness, high coherence, and potential compactness (Dudley et al., 2006). Recently the generation of ultrabroadband spectra through SC sources in the mid-infrared (MIR) region is of considerable interest because of their applications in the field of optical sensing, molecular fingerprint spectroscopy, bio-imaging, pulse compression, optical coherence tomography, and high precision frequency metrology (Aggarwal et al., 2002; Dudley et al., 2009 ; Andreasen et al., 2014). In the past years, numerous efforts were taken on silica fibers to produce broadband SC spectra which cover the visible and near-infrared regions (Ranka et al., 2000; Gao et al., 2012; Gao et al., 2012). However, silica fibers cannot be used in the MIR regime owing to their high losses in the spectral range beyond 3 μm which caused a gradual shift towards other types of glasses that posses large transmission windows having transparency into the long wavelength region. Alternative to fused silica, SC generation was also demonstrated using bismuth (Ebendroff-Heidepriem et al., 2004), lead silicate (Petropoulos et al., 2003), fluoride (Qin et al., 2009), tellurite (Domachuk et al., 2008; Liao et al., 2012; Agrawal et al., 2013), and ZBLAN fibers (Kulkarni et al., 2011).

Recently chalcogenide (ChG) glasses have shown a number of advantages over the other materials mentioned above due to their wider transmission window extending from 2 to 20 μm and higher nonlinearity into the MIR region (Eggleton et al., 2011). Such glasses are attractive for fabricating optical planar waveguides and microstructured based fibers owing to possessing low nonlinear absorption, low TPA, no FCA, and fast response time because of the absence of free-carrier effects. Moreover, ChG glass can provide MIR transparency up to 14 μm when selenide-based materials are employed and have third-order nonlinearity several hundred times larger than silica glass (Ma et al., 2013). Therefore, emphasised has given in most of the earlier theoretical and experimental investigation on chalcogenide based planar waveguides and step-index fibers for extending SC into the MIR region,but

the longest wavelength reached was limited owing to cladding absorption of step-index fiber (Kubat et al., 2014; Hudson et al., 2014; Petersen et al., 2014; Moller et al., 2015; Yu et al., 2015) and cut-off of the asymmetric nature of planar waveguide (Lamont et al., 2008; Gai et al., 2012; Yu et al., 2013; Yu et al., 2014; Karim et al., 2015) design. Photonic crystal fiber based design still attracts researcher attention much to employ it for MIR SC generation due to having no cladding absorption in the long wavelength edge and can be fabricated easily (Fatome et al., 2009; Hu et al., 2010; Weiblen et al., 2010; Wei et al., 2013). In our theoretical study, we show that the use of PCF instead of planar and conventional fibers can overcome this limitation and SC spectrum can be extended far into the MIR regime.

In this paper, we have shown through rigorous numerical investigations that a 3.6 cm long, dispersion engineered, $Ge_{11.5}As_{24}Se_{64.5}$ ChG PCF with hexagonal arrays of air-holes in its cladding can be used to generate a broadband SC with sufficient wavelength extension in the MIR regime. It was found in many previous experiment based works that for achieving sufficient extension of SC spectrum in the long wavelength region depends on the availability of pump pulses at a suitable wavelength, among other factors, and the pump wavelength needs to be around 4 μm or longer. To achieve ZDW of a PCF around such a long pump wavelength, the nonlinear coefficient of the PCF decreases due to decreasing effective mode area of the PCF. Therefore, to obtain longer wavelength extension of SC in the MIR region, higher pump powers are required which can cause damage to ChG PCF if relatively wide pump pulses are employed (Yu et al., 2013). Paying attention to this factor, we launched a fundamental mode with low peak power sub-picosecond sech pulses of 320 fs duration at a pump wavelength of 4 μm with a repetition rate of 21 MHz (Yu et al., 2014) in our numerical simulations. The attenuation (α) and nonlinear refractive index (n_2) are taken to be 0.5 dB/cm and 2.6×10^{-18} m^2/W, respectively (Ma et al., 2013; Yu et al., 2014). The nonlinear refractive index, n_2 was reduced by a factor of three at the pump wavelength of 4 μm from its measured value at 1.55 μm (Yu et al., 2014). The peak power of pulses is varied in the range 250-2000 W. A broadband MIR SC covering the wavelength range from 2 to 8 μm equivalent to 2 octave at the −15 dB level from the peak could be generated with our proposed ChG microstructured fiber. Our calculated bandwidths are the largest reported so far for SC generated using GeAsSe PCFs pumped at a wavelength of 4 μm with a low peak power of 2000 W.

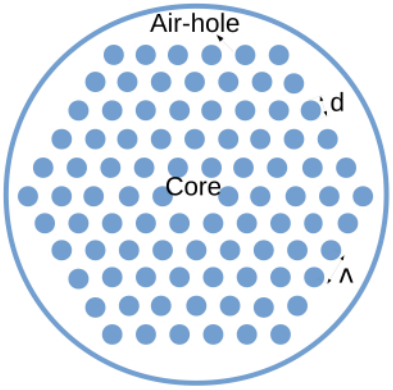

Figure 1. ChG PCF geometry used for dispersion optimization

2. Theory

Group velocity dispersion (GVD) and higher order dispersion parameters play a crucial role in determining the SC bandwidth at the PCF output. Ultrawide spectral broadening depends on how dispersion parameters interact with the nonlinearity of the PCF. The influence of a small anomalous GVD over a wide wavelength range produces a large soliton induced self frequency shifts through forming the Raman soliton inside the PCF. To realize PCF's zero-dispersion wavelength (ZDW) close to the pump wavelength, relatively larger waveguide dispersion is required to offset the material dispersion of ChG glasses. We use a finite element (FE) based full-vectorial mode-solver (Rahman et al., 1984) to obtain the propagation constant of the fundamental mode over a wide range of frequencies and to calculate the effective mode index, which is subsequently used for numerically evaluating GVD and various higher order dispersion parameters. The FE mode-solver used here is based on the vector **H**-field formulation that is one of the most accurate and numerically efficient approaches available for the solution of a wide

range of guided-wave problems. It can be easily applied to optical waveguides with any refractive index distribution and to those with anisotropic or nonlinear materials. The cross section of the waveguide is discretized using a large number of triangular elements. All three components of the magnetic fields can be represented as piece-wise polynomials within the elements. The field over each element is then expressed in terms of polynomials weighted by the fields over each element. By differentiating the functional with respect to each nodal value, the problem is reduced to a standard eigenvalue matrix equation, which is solved to obtain the propagation constants $\beta(\omega)$ and field profiles of various modes. In the full-vectorial formulation one needs to minimize the full **H**-field energy functional using (Rahman et al., 1984),

$$\omega^2 = \frac{\iint_\Omega \left[(\nabla \times \mathbf{H})^* . \hat{\varepsilon}^{-1} (\nabla \times \mathbf{H}) + p(\nabla . \mathbf{H})^* (\nabla . \mathbf{H})\right] d\Omega}{\iint_\Omega \mathbf{H}^* . \hat{\mu} \mathbf{H} \, d\Omega}, \tag{1}$$

where **H** is the vectorial magnetic field, * denotes a complex conjugate and transpose, ω is the angular frequency, p is a weighting factor for the penalty term to eliminate spurious modes, Ω is the computational domain of waveguide proposed, and $\hat{\epsilon}$ and $\hat{\mu}$ are the permittivity and permeability tensors, respectively.

Generalized nonlinear Schrödinger equation (GNLSE) can be solved for studing the process of SC generation inside our proposed ChG PCF. It is more important to include the dispersion parameters and intrapulse Raman scattering into GNLSE as accurately as possible during the modelling of SC generation in an optical waveguide. Therefore, the pulse evolutions in our proposed ChG PCF were modelled using GNLSE from (Gai et al., 2010):

$$\frac{\partial}{\partial z} A(z,T) = -\frac{\alpha}{2} A + \sum_{k \geq 2}^{10} \frac{i^{k+1}}{k!} \beta_k \frac{\partial^k A}{\partial T^k} + i\left(\gamma + i\frac{\alpha_2}{2A_{\text{eff}}}\right)\left(1 + \frac{i}{\omega_0}\frac{\partial}{\partial T}\right) \times \left(A(z,T) \int_{-\infty}^{\infty} R(T) \mid A(z, T - T') \mid^2 dT'\right), \tag{2}$$

where $A(z,T)$ is the slowly varying envelope of the pump pulse in a retarded time frame $T = t - \beta_1 z$ moving at the group velocity $1/\beta_1$, β_k ($k \geq 2$) is the kth order dispersion parameter, α accounts for linear propagation losses, and ω_0 is the pump angular frequency. The nonlinear coefficient is defined as $\gamma = n_2\omega_0/(cA_{\text{eff}})$, where n_2 is the nonlinear refractive index, c is the speed of light in vacuum, A_{eff} is the effective area of the mode at the pump frequency, and $\alpha_2 = 9.3 \times 10^{-14}$ m/W is the two-photon absorption coefficient (Gai et al., 2010). The material response function $R(t)$ includes both the instantaneous Kerr response, $\delta(t)$, and the delayed Raman response, $h_{\text{R}}(t)$, expressed as

$$R(t) = (1 - f_{\text{R}})\delta(t) + f_{\text{R}} h_{\text{R}}(t), \tag{3}$$

$$h_{\text{R}}(t) = \frac{\tau_1^2 + \tau_2^2}{\tau_1 \tau_2^2} \exp\left(-\frac{t}{\tau_2}\right) \sin\left(\frac{t}{\tau_1}\right). \tag{4}$$

where the parameter $f_{\text{R}} = 0.148$ represents the fractional contribution of the nuclei to the total nonlinear polarization.

3. Results and Discussions

To study SC generation, we solve GNLSE Eq. (2) for scalar calculations with single-polarization using split-step Fourier method including dispersion terms up to 10^{th} order. The design of a ChG PCF for SC generation depends on the accuracy of GVD and higher-order dispersion parameters. The accuracy of dispersion parameters depend on how accurately calculates the mode propagation, $\beta(\omega)$ for the fundamental mode through FE modal solutions. Therefore, accuracy of any design critically depends on the accuracy of modal solutions of a waveguide. For our ChG PCF, we represent the waveguide structure with 360,000 first order triangular elements to obtain higher accuracy modal solutions. A powerful extrapolation technique (Rahman et al., 1985) was then used to test the accuracy of modal solution for this waveguide structure. We tested the FE results by Aitken's extrapolation through convergence between the raw FEM results and extrapolated values as the number of elements increased. The mode propagation constant $\beta(\omega)$ of the fundamental mode over a range of frequencies are evaluated from the modal solutions obtained using the FE method described above. The effective indices ($n_{\text{eff}} = \lambda\beta(\omega)/2\pi$) of the fundamental mode are then calculated from the mode propagation constant obtained through modal solutions. The effective mode index of the fundamental mode is calculated up to fifteen decimal place so as to accurately determine the GVD and higher-order dispersion coefficients. The GVD curves obtained through FE mode-solver were tested by the data fitting method applying Taylor series expansion by which it was observed good matching

between the GVD curve obtained through both methods. The spatial profile of the fundamental mode at a pump wavelength of 4 μm, shown as an inset of Fig. 2(a), exhibits excellent field confinement to the central core region which thus enables an enhanced nonlinear interaction inside the ChG PCF.

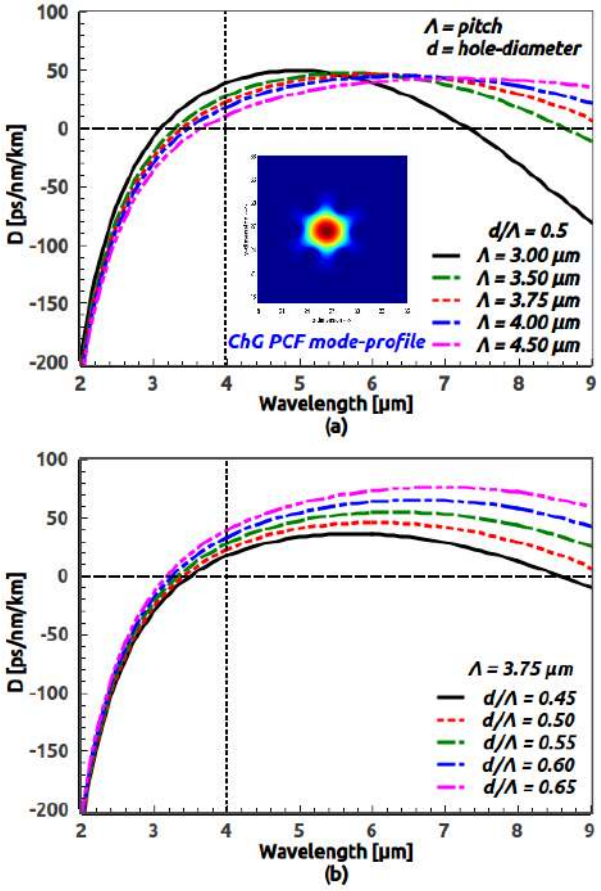

Figure 2. Dispersion curves for the ChG PCF design shown in Fig. 1 when (a) Λ is varied with d/Λ constant and (b) d/Λ is varied with Λ constant. Vertical dotted line indicates pump wavelength and the inset shows the spatial profile of the fundamental mode at a pump wavelength of 4 μm

PCF became popular since the first demonstration of Ranka *et al.,* (Ranka et al., 2000) as it has the ability to obtain large nonlinearity and flat GVD through microstructuring its cladding containing air holes around the pump wavelength for wideband SC generation. The ZDW of $Ge_{11.5}As_{24}Se_{64.5}$ ChG material is located near 7 μm and to shift this ZDW to shorter wavelengths, a number of techniques were proposed in (Hu et al., 2010; Weiblen et al., 2010; Wei et al., 2013). Here, we propose to design a $Ge_{11.5}As_{24}Se_{64.5}$ PCF and pump it at 4 μm using 320 fs pulses with a peak power of 2000 W from an optical parametric amplifier (Yu et al., 2014) to generate MIR SC that extends beyond 8 μm. We chose the PCF geometry because the ZDW of a PCF can be engineered over a much wider wavelength range compared to that of planar waveguides and step-index fibers. To shift the ZDW of a ChG PCF near 4 μm with a small value of anomalous dispersion at the pump wavelength, our proposed PCF structure for dispersion optimization is shown in Fig. 1. Its air holes follow hexagonal symmetry with the central air hole missing. Both the diameter (d) and pitch (Λ) of the air hole array can be varied to engineer PCF's dispersion properties. Through a rigorous numerical procedure, we obtain two sets of dispersion curves for our proposed PCF structure. Figure 2(a) shows how the dispersion curve $D(\lambda)$ changes when the pitch Λ is varied while keeping the ratio d/Λ constant. Figure 2(b) shows the situation in which the ratio d/Λ is changed while keeping Λ constant. These figures show that a ChG PCF can be designed to exhibit relatively small anomalous dispersion over a wide wavelength range extending from 3 μm to beyond 9 μm. For SC generation we need to pay attention on pump peak power as the ChG glass has the lowest damage threshold which is an average power density of 30 kW/cm^2. The damage threshold decreases when sulphide-based glass is progressively replaced with the selenium-based glass

(Yu et al., 2015). The ChG fiber core could be damaged if the peak intensity of pump pulses reaches 30 GW/cm^2 or the average power density at the input facet of the PCF exceeds 100 kW/cm^2. Considering these factors, we designed our GeAsSe PCF for MIR SC generation such that the required peak power of pump pulses is at most 2000 W. Among the many dispersion curves shown in Fig. 2 for our proposed ChG PCF structure, we chose the one with $\Lambda = 3.75$ μm and $d/\Lambda = 0.5$ (red-dotted line). The effective mode-area for these parameters is $A_{\text{eff}} = 17.61$ μm^2, resulting in a nonlinear coefficient $\gamma = 0.23$ W^{-1}/m and $D = 22.25$ ps/nm/km.

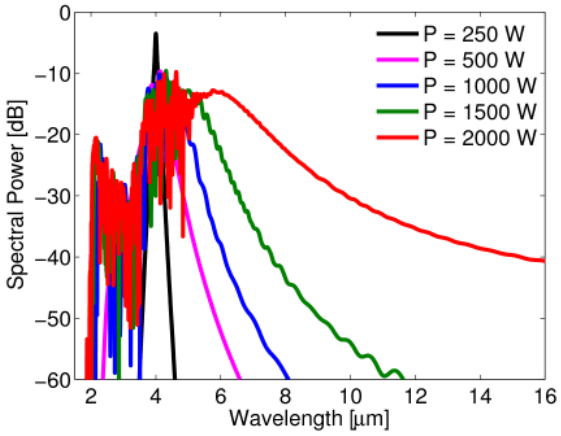

Figure 3. Simulated SC spectra when ChG PCF is pumped at a pump wavelength of 4 μm and the peak power of 320 fs pulses is varied from 250 to 2000 W

Evaluating higher-order dispersion terms up to 10$^{\text{th}}$ order at a pump wavelength of 4 μm from the red-dotted curve shown in Fig. 2(a) for $\Lambda = 3.75$ μm and $d/\Lambda = 0.5$, we have performed numerical simulations exciting fundamental mode propagating in the form of higher-order solitons with the peak power levels in the range between 250 and 2000 W, and the results are shown in Fig. 3. For the largest peak power of 2000 W, the SC spectrum at the PCF output clearly extends beyond 8 μm. To study how the SC evolves along the PCF length, we plot in Fig. 4 the evolution of pulse temporal (left) and spectral (right) density over the entire PCF length of 3.6 cm. The dispersion length of 320 fs pump pulse for our PCF is $L_{\text{D}} = 17.45$ cm, and the nonlinear length at a peak power of 2000 W is $L_{\text{NL}} = 2.2$ mm, resulting in a soliton order $N = \sqrt{L_{\text{D}}/L_{\text{NL}}} \approx 9$. As the pump lies in the anomalous GVD regime, SC generation is mainly dominated by the soliton-fission process. Initially the broadening of the optical pulse is dominated by self-phase modulation and then the propagation of pulse compressed due to the higher-order soliton dynamics. As a result, a broadened spectrum produced from strong temporal contraction. Further propagation now leads to a break-up of the higher-order soliton into a number of fundamental solitons through soliton fission process. For the soliton order of 9, fission occurs at around 1.5 cm as shown in Fig. 4(a), and nine fundamental solitons are produced after the fission, whose spectra shift toward the long-wavelength side owing to intrapulse Raman scattering, producing multiple spectral peaks in the spectra seen in Fig. 4(b). Since the generated solitons through fission process do not reach at the steady state instantaneously, the decay proceeds via bound soliton states with corresponding temporal contraction and expansion. One can see the non-solitonic radiation in the form of a dispersive wave is generated at a wavelength around 2 μm lying in the normal dispersion regime of our dispersion optimized photonic crystal fiber. It can be observed from Fig. 4(b) that the SC extends over more than 2 octaves covering a wavelength range from 2 μm to beyond 8 μm. The temporal and spectral differences are also apparent in the spectrogram shown in Fig. 5 and the SC extension beyond the 8 μm is clearly observed with a low peak power of 2000 W.

4. Conclusion

In conclusion, we have presented numerical study of 3.6-cm-long dispersion engineered ChG hexagonal PCF which allows us to generate ultrabroadband SC spectra in the MIR regime with a low peak power. We proposed here the microstructured fiber made with $Ge_{11.5}As_{24}Se_{64.5}$ glass and optimized its dispersive properties at the chosen pump wavelength by varying the pitch and diameter of air-holes which running periodically along the length of the PCF cladding. Using pump pulses at a wavelength of 4 μm with a relatively low peak power of 2 kW, we obtained a SC spectrum covering a wavelength range from 2 μm to beyond 8 μm (> 2 octave).

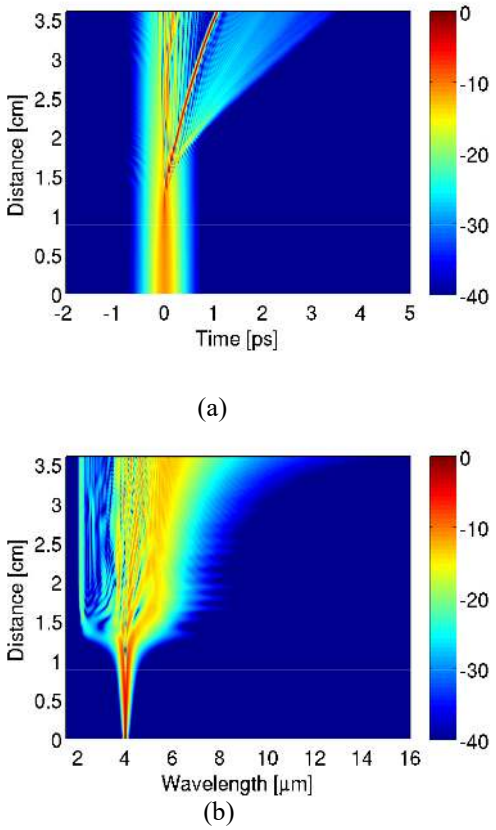

Figure 4. Output SC evolution of (a) temporal intensity and (b) spectral density along the PCF length for pump pulses launched at 4 μm with a peak power of 2000 W

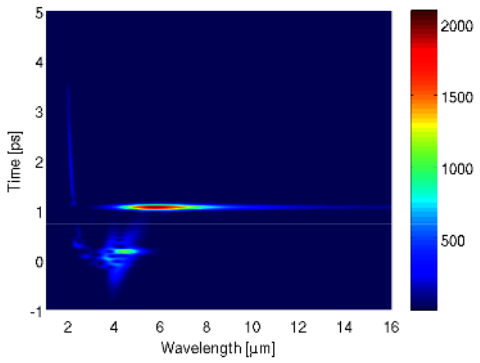

Figure 5. Temporal and spectral evolution of output SC presented by spectrogram for pump pulses launched at 4 μm with a peak power of 2000 W

This is the broadest MIR SC realized at a relatively low peak power of 2 kW using a GeAsSe based chalcogenide PCF so far reported. By shifting the pump wavelength to around 5-6 μm depending on the availability of the pump sources in this wavelength range, or increasing the pump power, or by adjusting both while paying attention to the damage threshold limit of ChG glass, it could be possible to extend the SC to beyond 14 μm with our proposed $Ge_{11.5}As_{24}Se_{64.5}$ chalcogenide glass photonic crystal fiber.

References

Aggarwal, I. D., & Sanghera, J. S. (2002). Development and applications of chalcogenide glass optical fibers at NRL. *J. Optoelectron. Adv. Mater., 4*(3), 665–678.

Agrawal, A., Tiwari, M., Azabi, Y.O., Janyani, V., Rahman, B. M. A., & Gratan, K. T. V. (2013). Ultrabroad supercontinuum generation in a tellurite equiangular spiral photonic crystal fiber. *J. of Modern Opt., 60*(12), 956–962. http://dx.doi.org/10.1080/09500340.2013.825334

Al-Kadry, A., Amraoui, M. E., Messaddeq, Y., & Rochette, M. (2014). Two octaves mid-infrared supercontinuum generation in As_2Se_3 microwires. *Opt. Exp., 22*(25), 31131–31137. http://dx.doi.org/10.1364/OE.22.031131

Andreasen, J., Bhal, A., & Kolesik, M. (2014). Spatial effects in supercontinuum generation in waveguides. *Opt. Exp., 22*(21), 25756–25767. http://dx.doi.org/10.1364/OE.22.025756

Domachuk, P., Wolchover, N. A., Cronin-Golomb, M., Wang, A., George, A. K., Cordeiro, C. M. B., Knight, J. C., & Omenetto, F.G. (2008). Over 4000 nm bandwidth of Mid-IR supercontinuum generation in subcentimeter segments of highly nonlinear tellurite PCFs. *Opt. Exp., 16*(10), 7161–7168. http://dx.doi.org/10.1364/OE.16.007161

Dudley, J. M., & Taylor, J. R. (2009). Ten years of nonlinear optics in photonic crystal fiber. *Nat. Photonics, 3*, 85–90. http://dx.doi.org/10.1038/nphoton.2008.285

Dudley, J. M., Genty, G., & Coen, S. (2006). Supercontinuum generation in photonic crystal fiber. *Rev. Mod. Phys., 78*, 1135–1184. http://dx.doi.org/10.1103/RevModPhys.78.1135

Ebendroff-Heidepriem, H., Petropoulos, P., Asimakis, S., Finazzi, V., Moore, R. C., Frampton, K., Koizumi, F., Richardson, D. J., & Monro, T. M. (2004). Bismuth glass holey fibers with high nonlinearity. *Opt. Exp., 12*(21), 5082–5087. http://dx.doi.org/10.1364/OPEX.12.005082 Eggleton, B. J., Luther-Davies,B., & Richardson, K. (2011). Chalcogenide photonics. *Nat. Photonics, 5*, 141–148. http://dx.doi.org/10.1038/nphoton.2011.309

Fatome, J., Fortier, C., Nguyen, T. N., Chartier, T., Smektala, F., Messaad, K., Traynor, N. (2009). Linear and nonlinear characterizations of chalcogenide photonic crystal fibers. *J. Lightwave Technol., 27*(11), 1707–1715. http://dx.doi.org/10.1109/JLT.2009.2021672

Gai, X., Choi, D., Madden, S., Yang, Z., Wang, R., & Luther-Devies, B. (2012). Supercontinuum generation in the mid-infrared from a dispersion-engineered As_2S_3 glass rib waveguide. *Opt. Lett., 37*(18), 3870–3872. http://dx.doi.org/10.1364/OL.37 .003870

Gai, X., Han, T., Prasad, A., Madden, S., Choi, D. Y., Wang, R., Bulla, D., & Luther-Davies, B. (2010). Progress in optical waveguides fabricated from chalcogenide glasses. *Opt. Exp., 18*(25), 26635–26646. http://dx.doi.org/10.1364/OE.18.026635

Gai, X., Madden, S, Choi, D. Y., Bulla, D., & Luther-Davies, B. (2010). Dispersion engineered $Ge_{11.5}As_{24}Se_{64.5}$ nanowires with a nonlinear parameter of 136 $W^{-1}m^{-1}$ at 1550 nm. *Opt. Exp., 18*(18), 18866–18874. http://dx.doi.org/10.1364 /OE.18.018866

Gao, W., Liao, M., Yan, X., Suziki, T., & Ohishi, Y. (2012). Mid-infrared supercontinuum generation in a suspended-core As_2S_3 chalcogenide microstructured optical fiber. *Appl. Opt., 51*(13), pp. 2346–2350. http://dx.doi.org/10.1364/OE.21.009573

Gao, W., Liao, M., Yang, L, Yan, X., Suziki, T., & Ohishi, Y. (2012). All-fiber broadband supercontinuum source with high efficiency in a step-index high nonlinear silica fiber. *Appl. Opt., 51*(8), pp. 1071–1075. http://dx.doi.org/10.1364/AO.51.001071

Granzow, N., Stark, S. P., Schmidt, M. A., Tverjanovich, A. S., Wondraczek, L., & Russell, P. St. J. (2011). Supercontinuum generation in chalcogenide-silica step-index fibers. *Opt. Exp., 19*(21), 21003–21010. http://dx.doi.org/10.1364/OE.19.021003

Hu, J., Menyuk, C. R., Shaw, L. B., Sanghera, J. S., & Aggarwal, I. D. (2010). Maximizing the bandwidth of supercontinuum generation in As_2Se_3 chalcogenide fibers. *Opt. Exp., 18*(3), 6722–6739. http://dx.doi.org/10.1364/OE.18.006722

Hudson, D. D., Baudisch, M., Werdehausen, D., Eggleton, B. J., & Biegert, J. (2014). 1.9 octave supercontinuum generation in a As_2S_3 step-index fiber driven by mid-IR OPCPA. *Opt. Lett.*, **39**(19), 5752–5755. http://dx.doi.org/10.1364/OL.39.005752

Karim, M. R., Rahman, B. M. A., & Agrawal, G. P. (2014). Dispersion engineered $Ge_{11.5}As_{24}Se_{64.5}$ nanowire for

supercontinuum generation: A parametric study. *Opt. Exp., 22*(25), 31029–31040. http://dx.doi.org/10.1364/OE.22.031029

Karim, M. R., Rahman, B. M. A., & Agrawal, G. P. (2015). Mid-infrared supercontinuum generation using dispersion-engineered $Ge_{11.5}As_{24}Se_{64.5}$ chalcogenide channel waveguide. *Opt. Exp., 23*(5), 6903–6914. http://dx.doi.org/10.1364/OE. 23.006903

Kubat, I., Petersen, C. R., Moller, U. V., Seddon, A. B., Benson, T. M., Brilland, L., Mechin, D., Moselund, P. M., & Bang, O. (2014). Thulium pumped mid-infrared 0.9-9 μm supercontinuum generation in concatenated fluoride and chalcogenide glass fibers. *Opt. Exp., 22*(4), 3959–3967. http://dx.doi.org/10.1364/OE.22.003959

Kulkarni, O. P., Alexander, V. V., Kumar, V., Freeman, M. J., Islam, M. N., Terry Jr., F. L., Neelakandan, M., & Chan, A. (2011). Supercontinuum generation from 1.9 to 4.5 μm in ZBLAN fiber with high average power generation beyond 3.8 μm using a thulium-doped fiber amplifier. *J. Opt. Soc. Am. B., 28*(10), 2486–2498. http://dx.doi.org/10.1364/JOSAB.28.002486

Lamont, M. R. E., Luther-Davies, B., Choi, D. Y., Madden, S., & Eggleton, B. J. (2008). Supercontinuum generation in dispersion engineered highly nonlinear (γ = 10 /W/m) As_2S_3 chalcogenide planar waveguide. *Opt. Exp., 16*(19), 14938–14944. http://dx.doi.org/10.1364/OE.16.014938

Lamont, M. R. E., Sterke, C. M., & Eggleton, B. J. (2007). Dispersion engineering of highly nonlinear As_2S_3 waveguides for parametric gain and wavelength conversion. *Opt. Exp., 15*(15), 9458–9463. http://dx.doi.org/10.1364/OE.15.009458

Liao, M., Gao, W., Duan, Z., Yan, X., Suzuki, T., & Ohishi, Y. (2012). Supercontinuum generation in short tellurite microstructured fibers pumped by a quasi-cw laser. *Opt. Lett., 37*(11), 2127-2129. http://dx.doi.org/10.1364/OL.37.002127

Mϕller, U., Yu, Y., Kubat, I., Petersen, C. R., Gai, G., Brilland, L., Mechin, D., Caillaud, C., Troles, J., Luther-Davies, B., & Bang, O. (2015). Multi-milliwatt mid-infrared supercontinuum generation in a suspended core chalcogenide fiber. *Opt. Exp., 23*(3), 3282–3291. http://dx.doi.org/10.1364/OE.23.003282

Ma, P., Choi, D. Y., Yu, Y., Gai, X., Yang, Z., Debbarma, S., Madden, S., & Luther-Davies, B. (2013). Low-loss chalcogenide waveguides for chemical sensing in the mid-infrared. *Opt. Exp., 21*(24), 29927–29937. http://dx.doi.org/10.1364/OE.21.029927

Petersen, C. R.. Mϕller, U., Kubat, I., Zhou, B., Dupont, S., Ramsay, J., Benson, T., Sujecki, S., Abdel-Moneim, M., Tang, Z., Furniss, D., Seddon, A., & Bang, O. (2014). Mid-infrared supercontinuum covering the 1.4-13.3 μm molecular fingerprint region using ultra-high NA chalcogenide step-index fiber. *Nat. Photonics, 8*, 830–834. http://dx.doi.org/10.1038/nphoton.2014.213

Petropoulos, P., Ebendroff-Heidepriem, H., Finazzi, V., Moore, R. C., Frampton, K., Richardson, D. J., & Monro, T. M. (2003). Highly nonlinear and anomalously dispersive lead silicate glass holey fibers. *Opt. Exp., 11*(26), 3568–3573. http://dx.doi.org/10.1364/OE.11.003568

Qin, G., Yan, X., Kito, C., Liao, M., Chaudhari, C., Suzuki, T., & Ohishi, Y. (2009). Ultrabroadband supercontinuum generation from ultraviolet to 6.28 μm in a fluoride fiber. *Appl. Phys. Lett., 95*(16), 161103. http://dx.doi.org/10 .1063/1.3254214

Rahman, B. M. A., & Davies, J. B. (19840). Finite-element solution of integrated optical waveguides. *J. Lightwave Technol., 2*, 682–688. http://dx.doi.org/10.1109/JLT.1984.1073669

Rahman, B. M. A., & Davies, J. B. (1985). Vector-H finite element solution of GaAs/GaAlAs rib waveguides. *In proceedings of IEE, 132*(6), 349–353. http://dx.doi.org/10.1049/ip-j:19850066

Ranka, J. K., Windeler, R. S., & Stentz, A. J. (2000). Visible continuum generation in air-silica microstructure optical fibers with anomalous dispersion at 800 nm. *Opt. Lett., 25*, 25–27. http://dx.doi.org/10.1364/OL.25.000025

Shaw, L. B., Gattass, R. R., Sanghera, J. S., & Aggarwal, I. D. (2011). All-fiber mid-IR supercontinuum source from 1.5 to 5 μm. *Proc. SPIE, 7914*. http://dx.doi.org/10.1117/12.877772

Silva, F., Austin, D. R., Thai, A., Baudisch, M., Hemmer, M., Faccio, D., Couairon, A., & Biegert, J. (20102). Multi-octave supercontinuum generation from mid-infrared filamentation in a bulk crystal. *Nat. Commun., 3*(807), 1–5. http://dx.doi.org/10.1038/ncomms1816

Wei, C., Zhu, X., Norwood, R. A., Seng, F., & Peyghambarian, N. (2013). Numerical investigation on high power mid-infrared supercontinuum fiber lasers pumped at 3 μm. *Opt. Exp., 21*(24), 29488–29504. http://dx.doi.org/10.1364/OE.21.029488

Weiblen, R. J., Docherty, A., Hu, J., & Menyuk, C. R. (2010). Calculation of the expected bandwidth for a mid-infrared supercontinuum source based on As_2S_3 chalcogenide photonic crystal fibers. *Opt. Exp., 18*(25), 26666–26674. http://dx.doi.org/10.1364/OE.18.026666

Yu, Y., Gai, X., Wang, T., Ma, P., Wang, R., Yang, Z., Choi, D., Madden, S., & Luther-Davies, B. (2013). Mid-infrared supercontinuum generation in chalcogenides. *Opt. Mater. Exp., 3*(8), 1075–1086. http://dx.doi.org/10.1364/OME.3.001075

Yu, Y., Gai, X., Zhai, C., Qi, S., Guo, W., Yang, Z., Wang, R., Choi, D., Madden, S., & Luther-Davies, B. (2015). 1.8-10 μm mid-infrared supercontinuum generation in a step-index chalcogenide fiber using low peak pump power. *Opt. Lett., 40*(6), 1081–1084. http://dx.doi.org/10.1364/OL.40.001081

Yu, Y., Zhang, B., Gai, X., Ma, P., Choi, D., Yang, Z., Wang, R., Debbarma, S., Madden, S., & Luther-Davies, B. (2014). A broadband, quasi-continuous, mid-infrared supercontinuum generated in a chalcogenide glass waveguide. *Laser Photonics Rev.*, pp. 1–7. http://dx.doi.org/10.1002/lpor.201400034

Copyrights